

# Linear stability in billiards with potential

Holger R. Dullin  
Institut für Theoretische Physik  
Universität Bremen  
Postfach 330440  
28344 Bremen, Germany  
Email: hdullin@physik.uni-bremen.de

## Abstract

A general formula for the linearized Poincaré map of a billiard with a potential is derived. The stability of periodic orbits is given by the trace of a product of matrices describing the piecewise free motion between reflections and the contributions from the reflections alone. For the case without potential this reduces to well known formulas. Four billiards with potentials for which the free motion is integrable are treated as examples: The linear gravitational potential, the constant magnetic field, the harmonic potential, and a billiard in a rotating frame of reference, imitating the restricted three body problem. The linear stability of periodic orbits with period one and two is analyzed with the help of stability diagrams, showing the essential parameter dependence of the residue of the periodic orbits for these examples.

PACS: 03.20.+i, 05.45.+b

## 1 Introduction

In the theory of dynamical systems billiards were introduced in the twenties of this century by Birkhoff. His idea was to have a simple class of models that show the complicated behavior of nonintegrable smooth Hamiltonian systems without the need to integrate a differential equation [1]: “But in this problem the formal side, usually so formidable in dynamics, almost completely disappears, and only the interesting qualitative questions need to be considered”. Birkhoff studied billiards inside smooth convex domains, for which it is now known [2] that they can not be ergodic. In the seventies Sinai proved the ergodicity of the billiard on a torus with a disk removed [3], and subsequently Bunimovich, Wojtkowski and others [4, 5] designed larger classes of ergodic billiards. Starting with some early papers in the eighties [6, 7] billiards became quite popular in physics. For investigations of both, the classical dynamics and the quantum mechanical properties, periodic orbits and their properties are of major interest, which are investigated using the Poincaré map.

For billiards the natural Poincaré map is from bounce to bounce: The boundary  $\partial\Omega$  of the billiard domain  $\Omega \subset \mathbb{R}^2$  is parametrized by the arc length  $s$ .  $\partial\Omega$  is assumed to be  $C^2$ , such that the curvature is well defined. Reflections at points in the boundary which are less smooth need a special treatment. Starting at some point  $\mathbf{r}(s_1) \in \partial\Omega$  all possible orbits leaving  $\partial\Omega$  can be parametrized by an angle  $\beta$  from  $-\pi/2$  to  $\pi/2$ , where  $-\pi/2$ ,  $0$ ,  $\pi/2$  specify the directions  $-\mathbf{t}(s_1)$ ,  $\mathbf{n}(s_1)$ ,  $\mathbf{t}(s_1)$  where  $\mathbf{t}(s_1)$  is the tangent vector to  $\partial\Omega$  at  $\mathbf{r}(s_1)$  and  $\mathbf{n}(s_1)$  is the normal vector pointing into  $\Omega$ . We have  $\partial_s \mathbf{r}(s) = \mathbf{t}(s)$  and  $\partial_s \mathbf{t}(s) = \kappa(s)\mathbf{n}(s)$  where  $\kappa(s)$  is the signed curvature at  $s$ , negative  $\kappa$  indicating a defocusing boundary with respect to  $\Omega$  or, equivalently, the normal  $\mathbf{n}$ . If instead of  $\beta$  the component  $p$  of the velocity parallel to  $\mathbf{t}$  is used,  $p = \sin \beta$ , then  $(s, p)$  are canonical coordinates on the Poincaré surface of section. The trajectory starting with  $\xi_1 = (s_1, p_1)$  encounters the boundary after time  $\tau$  at  $s_2$  and has a

parallel component  $p_2$  (with respect to  $\mathbf{t}(s_2)$ ) before and after the reflection. The Poincaré map is denoted by  $P$  such that  $P\xi_1 = \xi_2$ .

A periodic orbit of period  $n$  is now described by a list of points  $\xi_i = (s_i, p_i)$ ,  $i = 1, \dots, n$  such that  $P\xi_i = \xi_{i+1}$  for  $i = 1, \dots, n-1$  and  $P\xi_n = \xi_1$ , or equivalently  $P^n\xi_1 = \xi_1$ . Finding periodic orbits is a hard problem, even for billiards. In this paper we take the point of view that the periodic orbits are given to us, and we want to find a formula for their stability, i.e. for the linearized map  $DP$  of  $P$ .

In the following we will denote a quantity to be evaluated at  $\xi_i$  or  $s_i$  by a lower index  $i$ , e.g.  $\mathbf{r}(s_i) = \mathbf{r}_i$ ,  $\mathbf{t}(s_i) = \mathbf{t}_i$  or  $DP_{i,i+1}$  for the linearized map of  $P$  from  $\xi_i$  to  $\xi_{i+1}$ . Then we obtain for  $DP^n$

$$DP_{n,1}^n = DP_{n,n-1} \cdots DP_{32} DP_{21} \quad (1)$$

by the chain rule. For a smooth Hamiltonian system the linearized map depends on the solution of the variational differential equation, which can usually only be obtained by numerical integration. For an ordinary billiard without potential, rather than the infinite amount of information contained in this solution, we just need three numbers per reflection, besides the initial and final point: the time  $\tau$  (or length) between reflections, and the curvatures  $\kappa_i$  and  $\kappa_{i+1}$  of  $\partial\Omega$  at the initial and final points  $\mathbf{r}_i$  and  $\mathbf{r}_{i+1}$ . The expression of  $DP$  in terms of these data is well known, see e.g. [8, 9, 10]. The main point in stability formulas of this type is that they do *not* express everything in terms of the initial point  $\xi$ , which is of course possible. Instead, some quantities from the free motion, e.g. the time of flight  $\tau$ , directly enter the formula. The time  $\tau$  is usually given by the solution of a complicated equation (only for special boundaries can it be obtained from the roots of a polynomial of degree up to four). Therefore it makes sense (also numerically) to use  $\tau$  in stability formulas, because it must have been already calculated to obtain  $P$ .

If we add a simple potential to the billiard, the problem of the calculation of  $DP$  becomes a little harder. To keep the original idea of Birkhoff it only makes sense to add integrable potentials for which the solutions of the free motion in the potential can be written down explicitly. The general formula we obtain does not depend on the integrability, however in the examples we only treat integrable potentials. Typical examples are linear potentials [11, 12, 13, 14, 15, 9, 16] with free motion along parabolas, quadratic potentials [17, 9] with free harmonic motion, magnetic fields [18, 19] with free motion on circles and the fictitious forces of a rotating frame of reference [20]. The reason for the study of billiards with potential, besides of course the situation where they model a given physical situation, e.g. the restricted three body problem in [20], is that the potential can introduce two typical features of Hamiltonian systems which are absent in ordinary billiards. The most important is the energy dependence: As it is nicely illustrated in [15], one can observe the typical evolution from an integrable low energy limit, via an intermediate regime with the most complicated motion to an integrable high energy limit. This scenario is typical for bounded Hamiltonian systems, and billiards with potential are simple model systems of this kind. The second reason is that a magnetic field (or a rotating system) breaks the time reversal symmetry which is important because it influences the bifurcations of periodic orbits.

The paper is organized as follows. In sec. 2 we take a global point of view and discuss the topology of the surfaces of section induced by the potential. The linearized Poincaré map is obtained in sec. 3, and the results are used to calculate the stability of periodic orbits in sec. 4. In the remaining sections we calculate the stability of short periodic orbits for billiards with linear (sec. 5), quadratic or magnetic potential (sec. 6), and a rotating system, which models the restricted three body problem (sec. 7).

## 2 Billiards with potential

Let the Hamiltonian of the free motion be given by

$$H(\mathbf{q}, \mathbf{p}) = \frac{1}{2}(\mathbf{p} - \mathcal{A}(\mathbf{q}))^2 + U(\mathbf{q}). \quad (2)$$

The velocity is given by  $\mathbf{v} = \mathbf{p} - \mathcal{A}$ . In principle the calculation could be done with an additional positive definite “metric” in the kinetic energy, but in the application we have in mind we only need the above form. Let the configuration space of the free motion be  $\mathbb{R}^2$ . The energy surface of the billiard with potential is just the ordinary energy surface but with  $\mathbf{q}$  restricted to the interior of the billiard  $\Omega$ ,

$$\mathcal{E}_h = \{(\mathbf{q}, \mathbf{p}) \mid H(\mathbf{q}, \mathbf{p}) = h, \mathbf{q} \in \Omega\}. \quad (3)$$

Let the solution of Hamilton’s equations  $\dot{X} = \mathbf{J}\nabla X$  be given by the flow  $\phi$

$$\phi^t : X_1 \mapsto X(X_1; t), \quad (4)$$

where we introduced  $X = (\mathbf{q}, \mathbf{p})$  and the symplectic matrix  $\mathbf{J}$ . The section condition in our system is naturally given by the billiard boundary  $\partial\Omega \subset \mathbb{R}^2$  or explicitly by  $\mathbf{q}(t) = \mathbf{r}(s)$ , such that the surface of section  $\Sigma_h$  becomes

$$\Sigma_h = \{(\mathbf{q}, \mathbf{p}) \mid H(\mathbf{q}, \mathbf{p}) = h, \mathbf{q} \in \partial\Omega\}. \quad (5)$$

On the surface of section  $\Sigma_h$  we introduce coordinates  $\xi = (s, p)$ , where  $s$  is the arc length of  $\partial\Omega$  and  $p = \langle \mathbf{t}, \mathbf{v} \rangle$  is the component of the velocity  $\mathbf{v} = \mathbf{p} - \mathcal{A}(\mathbf{q}(s))$  parallel to the tangent vector  $\mathbf{t}(s)$ .<sup>1</sup> As we will see in the next section this is a canonical coordinate system on  $\Sigma_h$  and therefore  $P$  is area preserving in these coordinates. It is convenient to extend this coordinate system on  $\Sigma_h$  to the neighborhood of  $\Sigma_h$  in phase space. For this we take as local coordinates the energy  $h$  in the direction of  $\nabla H$ , and the time  $\mu$  in the direction of the flow  $\mathbf{J}\nabla H$ . The coordinate tuple  $(s, \mu, p, h)$  will be denoted by  $\Xi$ .

The Poincaré map  $P$  from bounce to bounce in a billiard with potential can now be described by a succession of four maps:

$$\begin{aligned} \sigma : \Xi_1 &\mapsto X_1 && \text{the map from the surface of section to phase space, } \Xi_1 = (s_1, 0, p_1, h) \\ \phi^{\tau_1} : X_1 &\mapsto \tilde{X}_2 && \text{the flow map of free motion in the potential} \\ \sigma^{-1} : \tilde{X}_2 &\mapsto \tilde{\Xi}_2 && \text{the map back to local coordinates on the surface of section} \\ \rho : \tilde{\Xi}_2 &\mapsto \Xi_2 && \text{the reflection, } \Xi_2 = (s_2, 0, p_2, h) \end{aligned} \quad (6)$$

The time  $\tau_1$  must be chosen in such a way that  $\tilde{X}_2 \in \Sigma_h$ , where the tilde denotes the moment before reflection, see below. As we will see, the description as a four dimensional mapping is convenient for the linearization of the map. If we write  $\sigma\xi$  we really mean  $\sigma\Xi$  where  $\Xi$  is the trivial 4-D extension of  $\xi$ , similarly for  $\sigma^{-1}$ .

In this notation the Poincaré map reads

$$\begin{aligned} P : \Sigma_h &\rightarrow \Sigma_h \\ \xi &\mapsto P(\xi) = \rho\sigma^{-1}\phi^\tau\sigma\xi; \end{aligned} \quad (7)$$

with  $\tau$  determined by  $\phi^\tau\sigma\xi \in \Sigma_h$ .

Note that if there is no reflection (i.e. if we study a Poincaré section of the free Hamiltonian)  $\sigma^{-1}$  from the last iteration and  $\sigma$  from the next cancel, such that the iterated map is given by

$$P^n\xi_1 = \sigma^{-1}\phi^{\tau_n} \dots \phi^{\tau_1}\sigma\xi_1 = \sigma^{-1}\phi^{(\tau_1+\dots+\tau_n)}\sigma\xi_1 \quad (8)$$

---

<sup>1</sup>Note that the  $p$  stands for parallel component of the *velocity*, not of the momentum  $\mathbf{p}$

as must be the case.

The tilde on  $\tilde{X}_2$  and  $\tilde{\Xi}_2$  indicates that we are on the surface of section but still in the instant before the reflection, such that the normal component  $\tilde{n}_2 = \langle \mathbf{n}_2, \tilde{\mathbf{v}}_2 \rangle$  of  $\tilde{\mathbf{v}}_2$  is smaller than 0. Here we take the point of view described in [21] that the surface of section consists of both parts with either sign of  $n_2$ . In the case of an ordinary billiard with a smooth boundary  $\Sigma_h$  becomes a 2-torus. This 2-torus is divided into two cylinders by the lines where the flow is tangent to the surface of section. They are given by the condition that the velocity  $\mathbf{v}$  is parallel (or anti parallel) to the tangent  $\mathbf{t}$ , or in local  $\mathbf{t}$ - $\mathbf{n}$ -coordinates by  $n = 0$ . In the case of a convex billiard these lines are two periodic orbits given by the clockwise and counterclockwise sliding motion along the boundary. One cylinder carries initial conditions with the velocity pointing inward (i.e. after the reflection,  $n > 0$ ) while on the other one the velocity is pointing outward (i.e. before the reflection,  $\tilde{n} < 0$ ). The flow  $\phi^\tau$  maps the first cylinder to the second, and the reflection  $\rho$  maps the second back to the first. In local  $\mathbf{t}$ - $\mathbf{n}$ -coordinates  $\rho$  is trivial: it just changes  $\tilde{n}$  to  $-n$ . This is the reason why we first use  $\sigma^{-1}$  and then  $\rho$ . Actually the points on  $\Sigma_h$  with outward pointing velocities can be considered the same points as the ones with the reflected inward pointing velocity, such that the reflection map gives an identification of the boundary of the filled torus  $\Omega \times S^1$ , which is the energy surface, and turns  $\mathcal{E}_h$  into a manifold without boundary. In the present case we obtain  $S^3$  by this construction.

If we add a potential the topological situation changes: the accessible region of motion in configuration space  $Q_h$  can now be a subset of the region  $\Omega$  bounded by the billiard walls. As usual  $Q_h$  is given by the condition  $U(\mathbf{q}) \leq h$ , such that for the billiard with potential we obtain

$$Q_h = \{\mathbf{q} | U(\mathbf{q}) \leq h, \mathbf{q} \in \Omega\}. \quad (9)$$

The additional boundaries  $\partial Q_h \setminus \partial \Omega$  are the ovals of zero velocity [1], where the kinetic energy vanishes due to the additional potential. Moreover there might be a subset of the energy surface, such that orbits in this subset never meet the boundary of  $\Omega$ . In the examples we are only dealing with integrable free Hamiltonians such that this part of the energy surface will be foliated by tori. Although the Poincaré section will be  $\mathcal{E}_h$ -incomplete [21], i.e. not every orbit in the energy surface will intersect  $\Sigma_h$ , the missing orbits are well under control and we ignore them in the following discussion. A very important point in adding a potential is that  $\mathcal{E}_h$ , the dynamics, and also  $\Sigma_h$  in general depend on the energy: instead of the entire  $\partial \Omega$  the part of the boundary in the accessible region of configuration space can now become a collection of intervals  $I \subset \partial \Omega$  if the energy is not too high. On every point of  $I$  we have a certain amount of kinetic energy available such that the norm of the velocity is fixed and all possible directions can be parametrized by an angle, such that we have to attach circles  $S^1$  to every point of  $I$ . However, at the boundaries of  $I$  where the ovals of zero velocity intersect the billiard boundary  $\partial \Omega$ , this circle has to be contracted to a point since the only possible velocity is 0. Therefore the surface of section becomes a collection of spheres, one for each interval in  $I$ . On each sphere there is a line where the velocity is tangent to  $\partial \Omega$ , and it divides the sphere into two disks. If we restrict our attention to the moment after reflection, the Poincaré map will be defined on this collection of disks.

### 3 The linearized map

For a general discussion of a Poincaré map from a (curved) surface in the energy surface to itself see e.g. [22, 23, 24]. As we will see, a symplectic coordinate system in the neighborhood of  $\Sigma_h$  is given by the arc length  $s$ , the parallel component  $p$  of the velocity  $\mathbf{v}$  (*not* of the momentum  $\mathbf{p}$ ), the value of the Hamiltonian  $h$ , and the flow time  $\mu$  starting at the point specified by  $s, p, h$ . Denote the components of this coordinate system by  $\Xi = (s, \mu, p, h)$ . The

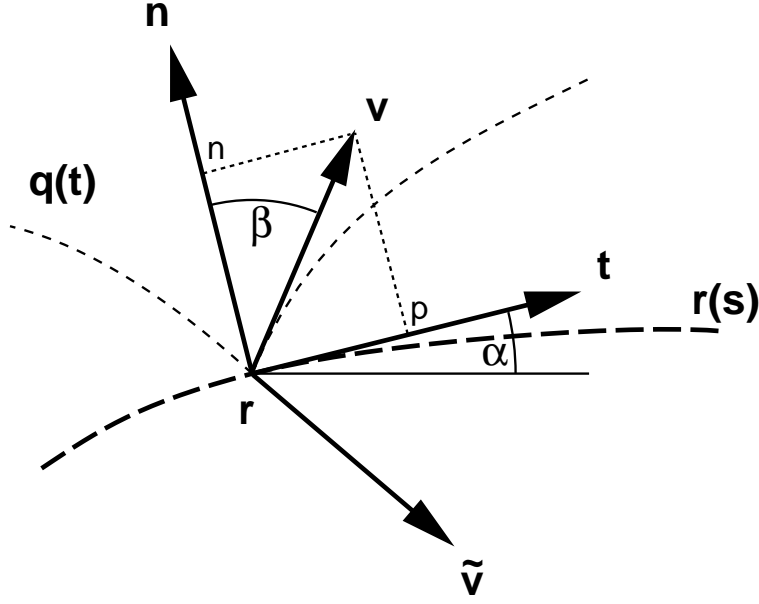


Figure 1: The orbit  $\mathbf{q}(t)$  encounters the boundary  $\partial\Omega$  given by the arc length parametrization  $\mathbf{r}(s)$  at  $\mathbf{r}$  with velocity  $\tilde{\mathbf{v}}$  before the reflection. The angle between the tangent  $\mathbf{t}$  at  $\mathbf{r}$  and a fixed horizontal reference direction is  $\alpha$ . The angle between the reflected velocity  $\mathbf{v}$  and the normal vector  $\mathbf{n}$  is  $\beta$ . In the  $\mathbf{t}$ - $\mathbf{n}$ -coordinate system the velocity  $\mathbf{v}$  is given by  $(p, n)$ , such that  $p = |\mathbf{v}| \cos \beta$ . Usually all quantities have an index to denote the point at which they are to be evaluated.

transformation to the original canonical variables  $X = (\mathbf{q}, \mathbf{p})$  is given by

$$X = \sigma \Xi = \phi^\mu F(s, p, h), \quad (10)$$

where  $F$  gives the initial point on  $\Sigma_h$  in the coordinates  $X$ . The position is given by  $\mathbf{q} = \mathbf{r}(s)$  and the velocity is  $\mathbf{v} = \mathbf{D}(\alpha(s))\mathbf{u}$  where  $\mathbf{u} = (p, n)$  is the velocity in the local  $\mathbf{t}$ - $\mathbf{n}$ -coordinate system and  $\mathbf{D} = (\mathbf{t}, \mathbf{n})$  the rotation matrix.  $\alpha$  is the angle between  $\mathbf{t}$  and the horizontal axis. To fix an orientation of the  $\mathbf{t}$ - $\mathbf{n}$ -system we let  $\mathbf{n}$  always point into  $\Omega$  and then rotate by  $\mathbf{S} = \mathbf{D}(\pi/2)$  to obtain  $-\mathbf{t} = \mathbf{S}\mathbf{n}$ . By this convention the curve  $\partial\Omega$  must be traversed counterclockwise for the billiard inside the curve and clockwise for the billiard outside the curve. This automatically fixes the sign of the curvature  $\kappa$  to be positive for the billiard inside a convex domain  $\Omega$ , and negative for the corresponding outer billiard.

The normal component  $n$  is implicitly defined via the shifted energy function on  $\Sigma_h$  given by

$$E(s, p, n, h) = \frac{1}{2}(p^2 + n^2) + U(\mathbf{r}(s)) - h, \quad (11)$$

where the positive square root gives  $n$  and the negative  $\tilde{n}$ . Now  $F$  is given by

$$F : (s, p, h) \mapsto X = (\mathbf{q}, \mathbf{p})^t = (\mathbf{r}(s), \mathbf{D}(\alpha(s))\mathbf{u} + \mathcal{A})^t. \quad (12)$$

We only want to know the transformation (10) close to  $\Sigma_h$ , i.e. for small  $\mu$  such that we can approximate  $\phi^\mu \approx \mathbf{1} + \mu \mathbf{J} \nabla H$ , where the Hamiltonian vector field  $\dot{X} = \mathbf{J} \nabla H$  at  $\mathbf{r}(s)$  in the coordinates  $X$  is needed,

$$\dot{X} = \begin{pmatrix} \dot{\mathbf{q}} \\ \dot{\mathbf{p}} \end{pmatrix} = \mathbf{J} \nabla H = \begin{pmatrix} \mathbf{v} \\ \langle \partial_q \mathcal{A}, \mathbf{v} \rangle - \partial_q U \end{pmatrix}. \quad (13)$$

The complete transformation, which gives  $\sigma$  for  $\mu = 0$ , is given by

$$X = F(s, p, h) + \mu \dot{X}|_{F(s, p, h)} = \begin{pmatrix} \mathbf{r} + \mu \dot{\mathbf{q}} \\ \mathbf{p} + \mu \dot{\mathbf{p}} \end{pmatrix}, \quad (14)$$

with  $\mathbf{p}$  and  $\dot{\mathbf{p}}$  given by (12,13) and  $n$  implicitly determined by (11). Now we want to find the linearization of this map at  $\mu = 0$  and show that it is a symplectic mapping. By this we find that the variables  $\xi = (s, p)$  are canonical on  $\Sigma_h$ . Moreover we need exactly this symplectic mapping to determine the linearized Poincaré map. Using (11) we obtain the derivatives of  $n$ . With the abbreviation  $\gamma = \langle \partial_q U, \mathbf{t} \rangle$  we find

$$\frac{\partial n}{\partial(s, p, h)} = -\frac{\partial E}{\partial(s, p, h)} \Big/ \frac{\partial E}{\partial n} = (-\gamma, -p, 1)/n. \quad (15)$$

The Jacobian of the transformation (14) at  $\mu = 0$  is the  $4 \times 4$ -matrix

$$\mathbf{L} = \frac{\partial X}{\partial \Xi} \Big|_{\mu=0} = (\partial_s F, \dot{X}, \partial_p F, \partial_h F) \quad (16)$$

$$= \begin{pmatrix} \mathbf{t} & \mathbf{v} & \mathbf{0} & \mathbf{0} \\ \partial_s \mathbf{p} & \dot{\mathbf{p}} & -\mathbf{S}\mathbf{v}/n & \mathbf{n}/n \end{pmatrix} =: \begin{pmatrix} \mathbf{A}_l & \mathbf{0} \\ \mathbf{C}_l & \mathbf{D}_l \end{pmatrix}, \quad (17)$$

$\mathbf{S} = \mathbf{D}(\pi/2)$ , and with (12) we find

$$\partial_s \mathbf{p} = (\partial_s \mathbf{D})\mathbf{u} + \mathbf{D}\partial_s u + \langle \partial_q \mathcal{A}, \partial_s \mathbf{r} \rangle \quad (18)$$

$$= \kappa \mathbf{S}\mathbf{v} - \mathbf{n}\gamma/n + \langle \partial_q \mathcal{A}, \mathbf{t} \rangle. \quad (19)$$

The symplectic condition,  $\mathbf{L}^t \mathbf{J} \mathbf{L} = \mathbf{J}$ , states that  $\mathbf{A}_l^t \mathbf{D}_l = \mathbf{1}$  and that  $\mathbf{A}_l^t \mathbf{C}_l$  be symmetric. The first holds because of  $\mathbf{t}^t \mathbf{n} = 0$ ,  $-\mathbf{v}^t \mathbf{S}\mathbf{v} = 0$  and  $\mathbf{v}^t \mathbf{n} = -\mathbf{t}^t \mathbf{S}\mathbf{v} = n$ , such that  $\mathbf{D}_l = \mathbf{A}_l^{-1t}$  and  $\det \mathbf{A}_l = n$ . The second condition is the identity

$$\langle \mathbf{v}, \partial_s \mathbf{p} \rangle = \langle \mathbf{t}, \dot{\mathbf{p}} \rangle \quad (20)$$

$$-\langle \mathbf{v}, \mathbf{n} \rangle \gamma/n + \langle \mathbf{v}, \partial_q \mathcal{A} \mathbf{t} \rangle = \langle \mathbf{t}, \partial_q \mathcal{A}^t \mathbf{v} \rangle - \langle \mathbf{t}, \partial_q U \rangle \quad (21)$$

$$-\gamma + \langle \mathbf{v}, \partial_q \mathcal{A} \mathbf{t} \rangle = \langle \mathbf{t}, \partial_q \mathcal{A}^t \mathbf{v} \rangle - \gamma. \quad (22)$$

The inverse of  $\mathbf{L}$  can be simply computed because  $\mathbf{L}$  is symplectic:

$$\mathbf{L} = \begin{pmatrix} \mathbf{A}_l & \mathbf{0} \\ \mathbf{C}_l & \mathbf{A}_l^{-1t} \end{pmatrix} \quad \mathbf{L}^{-1} = \begin{pmatrix} \mathbf{A}_l^{-1} & \mathbf{0} \\ -\mathbf{C}_l^t & \mathbf{A}_l^t \end{pmatrix}. \quad (23)$$

To linearize the Poincaré map we use  $\mathbf{L}|_{\xi_1} = \mathbf{L}_1$  to map vectors at  $\xi_1$  from  $T\Sigma_h$  to Euclidean coordinates, which are then mapped by the Jacobian of the flow  $\mathbf{M} = \partial \phi^t / \partial X$ . At the new point  $X_2$  we return to the section coordinates with  $\mathbf{L}^{-1}$  and keep in mind that we must still perform a reflection. In the local coordinate system this just means to put  $-n_2$  instead of  $\tilde{n}_2$  in  $\tilde{\mathbf{L}}_2^{-1}$ . To indicate this we write  $\tilde{\mathbf{L}}_i = \tilde{\mathbf{L}}(s_i, p_i, n_i) = \mathbf{L}(s_i, p_i, \tilde{n}_i) = \mathbf{L}(s_i, p_i, -n_i)$  such that

$$\frac{\partial \Xi_2}{\partial \Xi_1} = \tilde{\mathbf{L}}_2^{-1} \mathbf{M}_1 \mathbf{L}_1. \quad (24)$$

To obtain a  $2 \times 2$  matrix for  $DP$  we just set  $d\tau$  and  $dh$  equal to zero, i.e. we consider the restriction of the map to the tangent space  $T\Sigma_h$  in local coordinates on  $\Sigma_h$ . Deleting the appropriate rows and columns from  $\mathbf{L}$  and  $\mathbf{L}^{-1}$  we find

$$DP_{21} = \begin{pmatrix} -(\mathbf{S}\tilde{\mathbf{v}}_2)^t / \tilde{n}_2 & \mathbf{0} \\ -\partial_s \mathbf{p}_2^t & \mathbf{t}_2^t \end{pmatrix} \mathbf{M}_1 \begin{pmatrix} \mathbf{t}_1 & \mathbf{0} \\ \partial_s \mathbf{p}_1 & -\mathbf{S}\mathbf{v}_1/n_1 \end{pmatrix}, \quad (25)$$

where the left matrix is a  $2 \times 4$ -matrix and the right is a  $4 \times 2$ -matrix. For the trivial Hamiltonian of the ordinary billiard the only term in  $\partial_s \mathbf{p}$  is related to the curvature, see (19). In the presence of a potential  $U$  there is an additional contribution in the form of  $\gamma = \langle \partial_q U, \mathbf{t} \rangle$ , and a similar term  $\langle \partial_q \mathcal{A}, \mathbf{t} \rangle$  for the vector potential.

The Jacobian for the free motion in ordinary billiards is

$$\mathbf{M} = \begin{pmatrix} \mathbf{1} & \tau \mathbf{1} \\ \mathbf{0} & \mathbf{1} \end{pmatrix}, \quad (26)$$

and the main simplifications in this case come from the fact that  $\tilde{\mathbf{v}}_2 = \mathbf{v}_1$ , and with (19) we can rewrite (25) as

$$\begin{aligned} DP_{21} &= \begin{pmatrix} 1 & 0 \\ -\kappa_2 n_2 & 1 \end{pmatrix} \begin{pmatrix} -\mathbf{v}_2^t \mathbf{S} / n_2 & \mathbf{0} \\ \mathbf{0} & \mathbf{t}_2^t \end{pmatrix} \begin{pmatrix} \mathbf{1} & \tau \mathbf{1} \\ \mathbf{0} & \mathbf{1} \end{pmatrix} \begin{pmatrix} \mathbf{t}_1 & \mathbf{0} \\ \mathbf{0} & -\mathbf{S} \mathbf{v}_1 / n_1 \end{pmatrix} \begin{pmatrix} 1 & 0 \\ -\kappa_1 n_1 & 1 \end{pmatrix} \\ &= \begin{pmatrix} \frac{1}{n_2} & 0 \\ 0 & n_2 \end{pmatrix} \begin{pmatrix} 1 & 0 \\ -\frac{\kappa_2}{n_2} & 1 \end{pmatrix} \begin{pmatrix} -1 & -\tau \\ 0 & -1 \end{pmatrix} \begin{pmatrix} 1 & 0 \\ -\frac{\kappa_1}{n_1} & 1 \end{pmatrix} \begin{pmatrix} n_1 & 0 \\ 0 & \frac{1}{n_1} \end{pmatrix} \end{aligned} \quad (28)$$

which is a well known formula, see e.g. [8, 10]. For cases with potential more explicit formulas than (25) tend to be quite complicated. As we will see, it is nevertheless possible in some cases to perform the stability analysis up to period two. The obvious use of (25) is in the numerical calculation of Lyapunov exponents (see e.g. [10, 25]) and in the numerical search for periodic orbits with Newton's method. Note that if different, possibly non-canonical, coordinates are used, as the arc length parametrization of  $\partial\Omega$  may be too complicated, the expression for  $DP_{21}$  has to be sandwiched by the Jacobian of this transformation for Newton's method to work. Another application is the analytical estimation of the Lyapunov exponent as performed in [25]. Let us remark that the linearized map in the full phase space (24), besides being conceptually much clearer than (25), can be useful to implement a continuation method to find orbit cylinders in phase space, i.e. the collection of periodic orbits for different  $h$ , because it contains information about the change of the orbit if the energy changes.

## 4 Linear stability of periodic orbits

The standard application of the linearized map is to calculate the stability of periodic orbits. There is one simplification in calculating the stability of periodic orbits as compared to the calculation of the general linearized Poincaré map, namely that we are only interested in the trace of a product of linearized maps, and that we can cyclically permute matrices under the trace. The  $4 \times 4$  monodromy matrix  $\mathbf{M}_n^{(4)}$  of a period  $n$  orbit is given by

$$\mathbf{M}_n^{(4)} = \frac{\partial \Xi_1}{\partial \Xi_n} \frac{\partial \Xi_n}{\partial \Xi_{n-1}} \cdots \frac{\partial \Xi_2}{\partial \Xi_1} \quad (29)$$

and using (24) we obtain

$$\text{tr}_n^{(4)} := \text{tr} \mathbf{M}_n^{(4)} = \text{tr} \left( \tilde{\mathbf{L}}_1^{-1} \mathbf{M}_n \mathbf{L}_n \tilde{\mathbf{L}}_n^{-1} \mathbf{M}_{n-1} \mathbf{L}_{n-1} \cdots \tilde{\mathbf{L}}_2^{-1} \mathbf{M}_1 \mathbf{L}_1 \right). \quad (30)$$

Now we define the linearized reflection matrix

$$\mathbf{K}_i = \mathbf{L}_i^{-1} \tilde{\mathbf{L}}_i, \quad (31)$$

and with a cyclic permutation we find

$$\text{tr}_n^{(4)} = \text{tr} \prod_{i=1}^n \mathbf{M}_i \mathbf{K}_i. \quad (32)$$

The stability is split up into contributions from the reflection  $\mathbf{K}$  and from the free motion  $\mathbf{M}$ . Moreover, both contributions depend only on a single point, while for  $\frac{\partial \Xi_2}{\partial \Xi_1}$  we needed information about the initial and final point. A similar formula with  $2 \times 2$  matrices for the

ordinary billiard is well known, see e.g. [26, 27]. Multiplying  $DP_{32}DP_{21}$  as given by (28) we find

$$\cdots \begin{pmatrix} 1 & \tau_2 \\ 0 & 1 \end{pmatrix} \begin{pmatrix} -1 & 0 \\ 2\kappa_2/n_2 & -1 \end{pmatrix} \cdots \quad (33)$$

In (32) we have the natural generalization for an arbitrary billiard with potential, which is conveniently formulated in four dimensions.

The reflection matrix defined in (31) can be written as

$$\mathbf{K} = \begin{pmatrix} \mathbf{W} & \mathbf{0} \\ \mathbf{R} & \mathbf{W} \end{pmatrix}. \quad (34)$$

It is symplectic, which amounts to  $\mathbf{W}\mathbf{W}^t = \mathbf{1}$  and  $\mathbf{W}^t\mathbf{R}$  symmetric.  $\mathbf{W}$  is a symmetric involutive matrix with  $\det \mathbf{W} = -1$  and  $\mathbf{W}^2 = \mathbf{1}$ , as must be the case for a reflection:

$$\mathbf{W} = \begin{pmatrix} \cos 2\alpha & \sin 2\alpha \\ \sin 2\alpha & -\cos 2\alpha \end{pmatrix}. \quad (35)$$

The eigenvalue-eigenvector pairs of  $\mathbf{W}$  are  $(+1, \mathbf{t})$  and  $(-1, \mathbf{n})$ . The reflection line is  $\mathbf{t}$  and the direction of reflection is  $\mathbf{n}$ , recall that  $\alpha$  is the angle between  $\mathbf{t}$  and the horizontal axis. Note that the reflection  $\mathbf{W}$  acts on both, momenta and positions. In this way the mapping ‘‘corrects’’ the time at which the reflection took place: The symplectic coordinate system  $\Xi$  ensures that we do not have to bother to directly calculate the (linear approximation of the) change of time between reflections.

The lower left block  $\mathbf{R}$  of  $\mathbf{K}$  is much more complicated than the other blocks and contains all the contributions from  $\kappa$ ,  $U$  and  $\mathcal{A}$ . From (31) and (23) we find after some manipulations

$$\mathbf{R} = 2\frac{\kappa}{n}\mathbf{SDu}(\mathbf{SDW}_0\mathbf{u})^t + \frac{2}{n}\langle \partial_q U, \mathbf{n} \rangle \mathbf{nn}^t - \frac{4p}{n}B\mathbf{nn}^t + 4\langle \mathbf{n}, \partial_q \mathcal{A} \mathbf{t} \rangle \mathbf{S}, \quad (36)$$

where  $\mathbf{W}_0$  is the above reflection matrix at  $\alpha = 0$  and with  $\mathbf{q} = (x, y)$  we introduce  $B = \partial_x \mathcal{A}_y - \partial_y \mathcal{A}_x$ , the magnetic field. Except for the skew symmetric contribution from  $\partial_q \mathcal{A}$  the matrix  $\mathbf{R}$  is obviously singular. For constant magnetic fields we have  $\langle \mathbf{n}, \partial_q \mathcal{A} \mathbf{t} \rangle = B/2$ . In the following we will make this assumption, which is valid for the examples treated below. Note that  $\mathbf{SDW}_0\mathbf{u} = \mathbf{SWD}\mathbf{u} = \mathbf{SW}\mathbf{v}$  such that we obtain

$$\mathbf{R} = \frac{2\kappa}{n}\mathbf{Sv}(\mathbf{SWv})^t + \frac{2}{n}\langle \partial_q U, \mathbf{n} \rangle \mathbf{nn}^t - 2B\left(\frac{2p}{n}\mathbf{nn}^t + \mathbf{S}\right). \quad (37)$$

In the stability formulas we will often encounter

$$\text{tr} \mathbf{R} = \frac{2}{n}(\kappa(p^2 - n^2) + \langle \partial_q U, \mathbf{n} \rangle - 2pB), \quad R_{21} - R_{12} = 4\kappa p - 4B. \quad (38)$$

The monodromy matrix  $\mathbf{M}_n^{(4)}$  has eigenvalue 1 twice, with left eigenvector  $\nabla H$  and right eigenvector  $\mathbf{J}\nabla H$  [24, 28]. In the  $\Xi$  coordinate system it has the special form

$$\mathbf{M}_n^{(4)} = \begin{pmatrix} a & 0 & b & x \\ x & 1 & x & x \\ c & 0 & d & x \\ 0 & 0 & 0 & 1 \end{pmatrix} = \tilde{\mathbf{L}}_1^{-1} \mathbf{M}_n \mathbf{K}_n \cdots \mathbf{M}_1 \mathbf{K}_1 \mathbf{L}_1, \quad (39)$$

where  $x$  stands for arbitrary coefficients, and the entries  $a, b, c, d$  give the linearized  $2 \times 2$  Poincaré map  $DP^n$  in local coordinates. From  $\det \mathbf{M}_n^{(4)} = 1$  we see once more that  $\det DP = ad - bc = 1$ , such that  $\xi$  are area preserving coordinates for  $P$ . Right now we are interested in the fact that the spectrum of  $\mathbf{M}_n^{(4)}$  is  $\{1, 1, \lambda, 1/\lambda\}$  such that

$$\text{tr}_n^{(4)} = 2 + \lambda + \frac{1}{\lambda}. \quad (40)$$

By calculating  $\text{tr}_n^{(4)}$  we therefore obtain the eigenvalues of  $DP^n$ :

$$\text{tr}_n^{(2)} := \text{tr}DP^n = \text{tr}\mathbf{M}_n^{(4)} - 2 = \text{tr}_n^{(4)} - 2 = \lambda + \frac{1}{\lambda}. \quad (41)$$

## Period two orbits in the ordinary billiard

Let us now calculate  $\text{tr}_2^{(4)}$  for a period two orbit of the billiard without potential, where  $\mathbf{M}$  is given by (26). It will turn out that the same  $\mathbf{M}$  holds for the case of the gravitational billiard.

$$\text{tr}_2^{(4)} = \text{tr}(\mathbf{M}_2\mathbf{K}_2\mathbf{M}_1\mathbf{K}_1) \quad (42)$$

$$= 4\cos(2\alpha_1 - 2\alpha_2) + (\tau_1 + \tau_2)\text{tr}(\mathbf{W}_2\mathbf{R}_1 + \mathbf{R}_2\mathbf{W}_1) + \tau_1\tau_2\text{tr}\mathbf{R}_2\mathbf{R}_1 \quad (43)$$

For a period two orbit (without potential) we have  $p_1 = p_2 = 0$ ,  $n_1 = n_2 = 1$ ,  $\tau = \tau_1 = \tau_2$  and  $\alpha_1 = \alpha_2 + \pi$ , hence we obtain

$$\text{tr}_2^{(4)} = 4 - 4\tau(\kappa_1 + \kappa_2) + 4\kappa_1\kappa_2\tau^2, \quad (44)$$

which is a well known result, see e.g. [9]. Before passing to the new application to gravitational billiards, we show the stability diagram of this period two orbit. It is convenient to introduce Greene's residue  $R$  [29] and its "complement"  $\bar{R}$  defined by

$$\bar{R} = 1 - R = \text{tr}^{(4)}/4, \quad (45)$$

such that in the above case

$$1 - R = \bar{R} = (1 - \tau\kappa_1)(1 - \tau\kappa_2). \quad (46)$$

Bifurcations with  $\lambda = +1$ ,  $R = 0$  are called "direct parabolic" and bifurcations with  $\lambda = -1$ ,  $\bar{R} = 0$  "invers parabolic". The direct parabolic bifurcation with  $\lambda = 1$  generically means the creation of periodic orbits "out of nothing" in a saddle-center bifurcation. Thus, the continuous dependence of orbits on the bifurcation parameter is not guaranteed at this point. Index preservation [30] requires the simultaneous creation of one orbit with index +1, which must be elliptic close to  $R = 0$ , and one orbit with index -1 which is always direct hyperbolic. In the presence of symmetry (e.g. time reversal symmetry) a symmetric orbit may depend continuously on the bifurcation parameter, and in this case one observes a symmetry breaking pitch fork bifurcation instead [31].

At an invers parabolic bifurcation with  $\lambda = -1$ ,  $\bar{R} = 0$  the periodic orbit depends continuously on the bifurcation parameter, and this is the most important difference as compared to the direct parabolic case. The orbit has index +1, and there is no way to create an orbit with the same period  $n$  and index -1 because  $R = 1$ . Therefore the orbit must survive the crossing of the line  $R = 1$ , and turns from elliptic via invers parabolic to inverse hyperbolic. However, considering the map  $P$  iterated  $2n$  times, an inverse hyperbolic orbit of period  $n$  looks hyperbolic, such that we have index -1 for  $P^{2n}$ , and therefore we typically expect the creation of two stable orbits of period  $2n$  with index +1 (or the destruction of two unstable ones). This is called period doubling bifurcation. Of course there can be more complicated bifurcations at  $\lambda = \pm 1$ , and also additional resonances in the elliptic region, see e.g. [30, 32].

In Fig. 2 we show the level lines of  $R$  as a function of  $\tau\kappa_1$  and  $\tau\kappa_2$ . We could scale the length by  $\tau$  such that we always deal with a unit length orbit, but sometimes it is more natural to think of an orbit as becoming longer instead of the curvature becoming larger. Regions with elliptic orbits ( $0 < R < 1$ ) are shaded. The boundaries are given by  $R = 0$  (i.e. by the hyperbola  $\tau = 1/\kappa_1 + 1/\kappa_2$ ), the direct parabolic case, and by the two lines  $\bar{R} = 0$  with  $\tau\kappa_1 = 1$  or  $\tau\kappa_2 = 1$ , the invers parabolic case. The interpretation is as follows, where

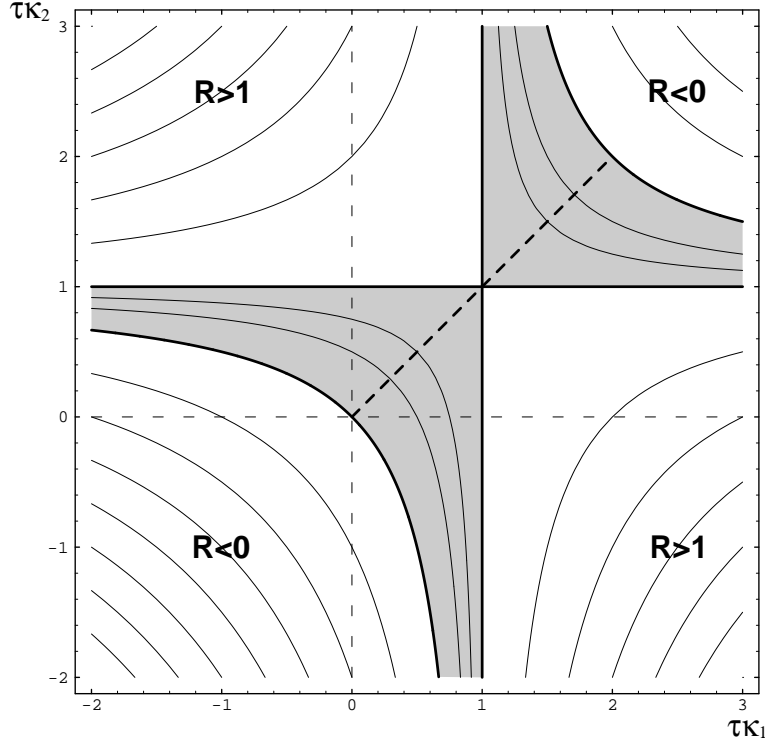


Figure 2: Stability diagram for period two orbits in the billiard without potential. Contour lines of the residue  $R$  (46) are shown. The elliptic region is shaded. Inside this region the lines with  $R = 1/2, 3/4$  are drawn. In the unstable regions the integer valued residues are shown. The bold dashed line indicates the stable period two orbit in the family of billiards with elliptic boundary. Period two orbits of the Sinai billiard are in the lower left quadrant, those of the stadium billiard, or the unstable ones in the ellipse, are in the upper right region with  $R < 0$ . With an appropriate change of the axes labeling this diagram can also be used for period two orbits of the billiard in a constant magnetic field (56) and for period one and period two orbits of the billiard with a harmonic potential (65,66,67).

due to symmetry we restrict the discussion to  $\tau\kappa_2 > \tau\kappa_1$ :

If both boundaries at the reflection points are defocusing,  $\kappa_i < 0$ , the orbit is unstable. The direct parabolic reflection at two parallel straight lines is at the upper right corner of this quadrant. If there is one focusing and one defocusing reflection the orbit is usually inverse hyperbolic; however, even for large defocusing curvature, elliptic motion is always possible. If we lower the value of  $\tau\kappa_2$  starting in the inverse hyperbolic region we will encounter an inverse parabolic bifurcation at  $\tau\kappa_2 = 1$ . Then there is a small elliptic region which we leave via a direct parabolic bifurcation. There is no further bifurcation if the boundary becomes defocusing.

The region with two focusing reflections,  $\kappa_i > 0$ , is the most complicated. If the orbit is sufficiently long, then it is direct hyperbolic,  $R < 0$ . This is the longer period two orbit that is always present in a smooth convex billiard. If we make the orbit shorter we encounter a direct parabolic bifurcation if  $\tau\kappa_1$  is sufficiently close to 1. Examples of orbits in the intermediate stable region are the shorter period two orbit of smooth convex billiards (if they are stable). At  $\tau\kappa_1 = 1$  these orbits become inverse hyperbolic if the curvatures are different, even though both reflections are focusing. However if the length is decreased further the orbit becomes stable again at  $\tau\kappa_2 = 1$ .

The period two orbit of the circle billiard is at  $\tau\kappa_1 = \tau\kappa_2 = 2$ , and for an ellipse with semi major axes  $a$  and  $b$ ,  $a > b$  the unstable orbit along the longer axis is at  $\tau\kappa_i = 2a^2/b^2$  while the stable one is at  $\tau\kappa_i = 2b^2/a^2$ , indicated by the bold dashed line. For  $a = b\sqrt{2}$  it is invers

parabolic, such that this situation is particularly susceptible to perturbations. Note that the passage of the stable periodic orbit of an integrable system through the special point where the two regions of elliptic motion meet,  $\kappa_1 = \kappa_2$ , avoids additional bifurcations. We will see the same behavior in the integrable billiard with parabolic boundary in a gravitational field.

## 5 The gravitational billiard

In the gravitational billiard we have a linear potential  $U = \langle \mathbf{g}, \mathbf{q} \rangle$  with  $\mathbf{g} = (0, g)^t$ . Using the Jacobian  $\mathbf{M}$  of the free motion

$$\mathbf{M} = \frac{\partial X(t)}{\partial X_1} = \begin{pmatrix} \mathbf{1} & t\mathbf{1} \\ \mathbf{0} & \mathbf{1} \end{pmatrix} \quad (47)$$

the general solution is given by

$$X(t) = \mathbf{M} \begin{pmatrix} \mathbf{q}_1 \\ \mathbf{p}_1 \end{pmatrix} - \begin{pmatrix} t^2 \mathbf{g}/2 \\ t\mathbf{g} \end{pmatrix}. \quad (48)$$

$\mathbf{M}$  is the same as for the ordinary billiard without potential. In this system a period one orbit exists if there is a point on the boundary with horizontal tangent, such that  $\mathbf{q}(\tau) = \mathbf{q}_1$  and  $\mathbf{p}(\tau) = -\mathbf{p}_1$ . Their trace is given by

$$\text{tr}_1^{(4)} = \text{tr} \mathbf{M} \mathbf{K} = \text{tr}(2\mathbf{W} + \tau \mathbf{R}) = \tau \text{tr} \mathbf{R} \quad (49)$$

and with  $\mathbf{t} = (1, 0)$ ,  $\mathbf{n} = (0, 1)$  and  $p = 0$  we obtain from (38) that

$$\text{tr}_1^{(4)} = 2\tau(-\kappa n + g/n) = 4 - 2\kappa\tau n. \quad (50)$$

In the latter equations we used  $\tau = 2n/g$  to eliminate  $g$  from the expression. With  $h = n^2/2$  and eliminating  $\tau$  we find  $\text{tr}_1^{(2)} = 2 - 8\kappa h/g$ , which is well known, see e.g. [16, 9]. Additional relations like  $\tau g = 2n$  in this simple example, exist between the quantities entering the stability formulas, because we have circumvented the use of the solution of the equations of motion. The additional relations appear in the monodromy matrix in the  $\Xi$  coordinate system: It must have the form (39), i.e. the 0's and 1's are always there. In more complicated applications it might be more appropriate to calculate these relations directly, but the final check with (39) should always be made.

The interpretation of the bifurcation of the periodic orbit is as follows: If the boundary is defocusing, as e.g. studied in [33], the orbit is direct hyperbolic. At a flat boundary we have a direct parabolic bifurcation. For a focusing boundary the orbit is elliptic for small energies and becomes inverse hyperbolic if the energy becomes large compared to the radius of curvature. The inverse parabolic transition at  $g = 2h\kappa$  typically creates an elliptic period two orbit in a period doubling bifurcation. Now we turn to the calculation of the stability of the period two orbit created in this bifurcation. We only treat the case of the time and space symmetric period two orbit. The spatial symmetry is a reflection at the vertical axis, such that the angles  $\alpha_i$  between the tangent at the reflection points and the horizontal axis are related by  $\alpha_2 = -\alpha_1$ . The time reversal symmetry requires  $p_1 = p_2 = 0$ .

Instead of calculating the full symmetric periodic two orbit we introduce an upright wall at the place of the vertical symmetry axis for which again  $p_2 = 0$  must hold. The reflection matrix  $\mathbf{K}_2$  for this wall with  $\alpha_2 = \pm\pi/2$  and  $\kappa_2 = 0$  is given by

$$\mathbf{K}_2 = \begin{pmatrix} \mathbf{W}_0 & \mathbf{0} \\ \mathbf{0} & \mathbf{W}_0 \end{pmatrix}. \quad (51)$$

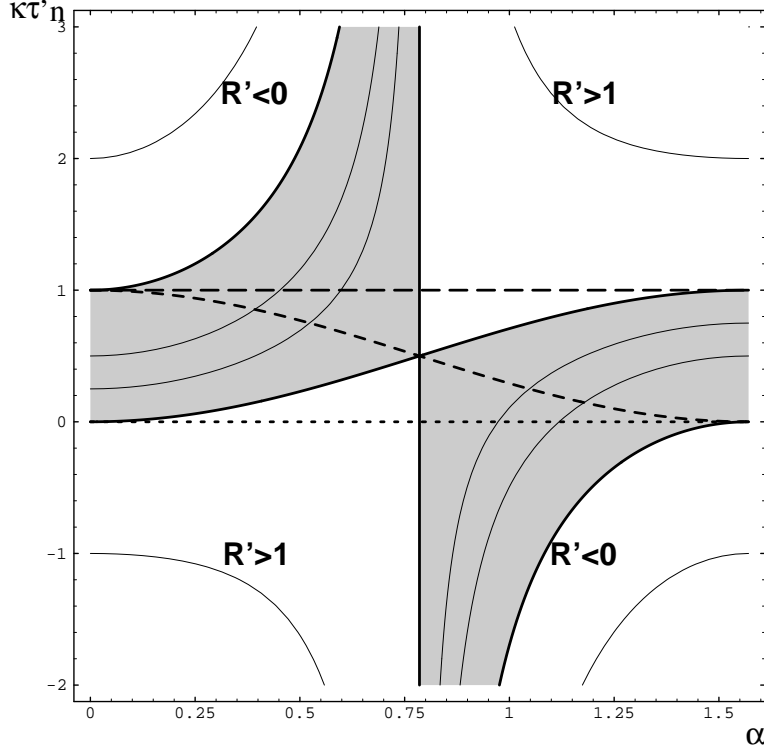


Figure 3: Stability diagram for the symmetry reduced period two orbit in the gravitational billiard. The contour lines of the residue  $R' = 1 - \bar{R}'$  (53) are shown. The elliptic region is shaded. Inside this region the lines with  $R' = 1/2, 3/4$  are shown. In the unstable regions the integer valued residues are shown. The dashed line indicates the stable periodic orbit in the family of billiards in the paraboloid. The dotted line corresponds to the wedge billiard and the long dashed line to the circle billiard.

Formula (42) is also valid for the gravitational billiard because it has the same Jacobian as the ordinary billiard, and it reduces to

$$\frac{\text{tr}_2^{(4)}}{4} = \cos(2\alpha \pm \pi) + \frac{\tau'}{2} \text{tr}(\mathbf{W}_0 \mathbf{R}_1) = -\cos 2\alpha + \frac{\tau'}{n} \cos 2\alpha (\kappa n^2 + g \cos \alpha). \quad (52)$$

The time  $\tau'$  is just half the time of the full orbit. Using the relation  $g\tau' = n \cos \alpha$  obtained from the explicit solution with the above boundary values, we find

$$1 - R' = \bar{R}' = \cos 2\alpha (n\kappa\tau' - \sin^2 \alpha) \quad (53)$$

The residue for the full orbit is now obtained from

$$1 - R = \bar{R} = (1 - 2\bar{R}')^2. \quad (54)$$

The reason that the residue (or its complement) factorize in the above fashion is usually related to a symmetry in the system. If we shift the zero of the potential energy to the initial point we can again use  $h = n^2/2$  to eliminate  $\tau$ .

Let us now study the stability of this periodic orbit in a diagram similar to Fig. 2. Recall that we are not discussing the question of existence of the orbit. In fact this orbit (even in symmetric boundaries) does not exist for all energies. But if it exist, its stability can be read off Fig. 3, where the residue  $R' = 1 - \bar{R}'$  of the symmetry reduced orbit is plotted as a function of  $n\kappa\tau'$  and  $\alpha$ . We start by analyzing classes of orbits with constant angles  $\alpha = 0, \pi/2, \pi/4$ .

For  $\alpha = 0$  we have the orbit bouncing up and down on a vertical line. This is not, however, the period one orbit discussed above, because there is also an upper wall. The residue is just

$1 - n\kappa\tau'$ . For infinite energies this line describes periodic orbits of the billiard without potential. To compare to Fig. 2 we must pass to the unreduced system with  $R = 4R'(1 - R')$  and  $\tau = 2\tau'$ . Then the line  $\alpha = 0$  can be mapped to the diagonal of Fig. 2.

In the other extreme we have  $\alpha = \pi/2$  which means a reflection at a vertical wall with  $R' = n\kappa\tau'$ . This motion can only be realized for infinite energies or vanishing distance and we can connect this line to the period two orbit in the billiard without potential: the residue of the full system on the line  $\alpha = \pi/2$  can again be mapped to the diagonal of Fig. 2.

There is the surprising feature that at  $\alpha = \pi/4$  the orbits are inversely parabolic, *independently* of all the other quantities. For an intuitive explanation consider the non-symmetry reduced system: to throw a ball the farthest distance with least energy it must take off with an angle of  $\pi/4$ . For higher energies and the same distance there are two distinct solutions, the higher orbit taking a longer time than the lower one. Together these two orbits together give a period two space symmetric orbit which does not possess time reversal symmetry. In the full system the time symmetric orbits have residue 0, and we have a symmetry breaking pitch fork bifurcation, which appears as a period doubling bifurcation in the reduced system.

Let us now look at orbits with arbitrary angle  $\alpha$  and defocusing boundary,  $n\kappa\tau' < 0$ . For  $\alpha < \pi/4$  the orbits are always inverse hyperbolic (in the reduced system). Note that in the full system the symmetric period two orbit is always direct hyperbolic if it is unstable. If the angle is increased beyond  $\pi/4$  the defocusing boundary orbit always becomes first elliptic and eventually direct hyperbolic as the ordinary billiard at  $\alpha = \pi/2$  is approached. For a focusing boundary ( $n\kappa\tau' > 0$ ) the orbit is (almost) always stable at  $n\kappa\tau' = 1/2$ . We observe that the whole picture is invariant under a rotation by  $\pi$  around the point  $(\pi/4, 1/2)$ . With this duality we can translate the statement “defocusing boundary for small angles is inverse hyperbolic” to “sufficiently focusing boundary and large angles is inverse hyperbolic”, and similarly “sufficiently focusing boundary and small angle is hyperbolic”.

Now we discuss the evolution of this orbit in specific examples. The creation of the period two orbit by period doubling from the upright bouncing motion happens at  $\alpha = 0$ ,  $n\kappa\tau = 1$  with residue 0. This point is part of two well known billiards, the integrable parabola billiard [9, 16] and the (gravitational) billiard inside the circle [15]. The line of the period two orbits of these systems, parametrized, e.g., by the energy, is also given in Fig. 3. In the circle billiard  $n\tau$  is constant ( $\kappa$  is trivially a constant). For small energies (and therefore angles) the orbit is stable, at  $\alpha = \pi/4$ , it becomes unstable in a period doubling bifurcation and stays unstable henceforth. At infinite energy the billiard becomes the integrable circle billiard without potential and the period two orbit is direct parabolic. For the parabola billiard the behavior is quite different. The creation of the orbit starts at the same place, but according to the already stated observation that integrable systems avoid bifurcations it stays in the elliptic region when the angle and energy are increased, passes to the symmetry point of the diagram and stops at the infinite energy limit. The third line shown in Fig. 3 corresponds to the period two orbit in the wedge billiard [11, 12], for which the curvature is zero. At  $\alpha = \pi/2$  this line joins the one of the parabola billiard. Here, however, we do not have an infinite energy limit but instead zero distance: The angle  $\alpha$  is also the wedge angle, which is the only system parameter, and at  $\pi/2$  the wedge degenerates into a line. For  $\alpha > \pi/4$  the orbit is elliptic, at  $\pi/4$  where the billiard becomes integrable it is inversely parabolic and for smaller angles it is inverse hyperbolic, as must be the case because the billiard is ergodic for  $\alpha < \pi/4$  [34].

Let us finally remark that the above stability formula for the full orbit is quite similar if the curvatures are different at the reflection points,  $\bar{R} = (1 - 2\bar{R}'_1)(1 - 2\bar{R}'_2)$ , where  $\bar{R}'_i$  is given by (53) with the curvature  $\kappa$  replaced by  $\kappa_i$ .

## 6 Billiards with constant magnetic field or harmonic potential

The stability formulas for the symmetric period two orbits in the billiard with harmonic potential or magnetic field are structurally similar to those of the ordinary billiard. In the symmetric case of the ordinary billiard we find from (46) that  $R = 2\kappa l(1 - \kappa l/2)$  where  $l$  is the length of the orbit. The factor  $1 - \kappa l/2$  will turn out to be present in the following examples with potential, such that its geometric significance is independent of the additional potential: If the Euclidean distance of reflection points is equal to the diameter of a circle with radius (of curvature)  $1/\kappa$  the stability changes.

### Constant magnetic field

The vector potential of the constant magnetic field  $B$  is  $\mathcal{A} = (-yB/2, xB/2)$ , where we denoted the components of  $\mathbf{q}$  by  $(x, y)$ . The free motion takes place on circles with Larmor radius  $|\mathbf{v}|/|B|$ . The Jacobian of the free motion is given by

$$\mathbf{M}(t) = \begin{pmatrix} (\mathbf{1} + \mathbf{D}(Bt))/2 & -(\mathbf{1} - \mathbf{D}(Bt))\mathbf{S}/B \\ B(\mathbf{1} - \mathbf{D}(Bt))\mathbf{S}/4 & (\mathbf{1} + \mathbf{D}(Bt))/2 \end{pmatrix}, \quad (55)$$

where  $\mathbf{D}(Bt)$  is a rotation matrix, which will always be written with its argument to distinguish it from the rotation  $\mathbf{D}$  around the angle  $\alpha$ . The general solution is just given by  $X(t) = \mathbf{M}(t)X(0)$ . We take  $B < 0$  such that the particles rotate counterclockwise.

Since the circles of the free motion are already periodic orbits the billiard does not have period one orbits. For a period one orbit we need a free orbit that returns to the initial point in configuration space, but with different velocities. The billiard wall is then adjusted in such a way that the final velocity is reflected to the initial one. We again restrict ourselves to a symmetric period two orbit, i.e.  $\alpha_2 = \alpha_1 + \pi$ . Because of isotropy of space we can set  $\alpha_1 = 0$  and  $\alpha_2 = \pi$  (the same argument could have been used for the billiard without potential), such that  $\mathbf{W}_2 = \mathbf{W}_1 = \mathbf{W}_0$ , where the last index denotes the standard reflection matrix ( $\alpha = 0$  in (35)), not the position of reflection. Using the relation  $2\beta = |B|t$ , where  $2\beta$  is the angle of the part of the circle traveled by the free orbit to eliminate the time, such that  $p = |\mathbf{v}| \cos \beta$  and  $n = |\mathbf{v}| \sin \beta$ , we find

$$\bar{R} = (1 + 2p/B\kappa_1)(1 + 2p/B\kappa_2). \quad (56)$$

Noting that the Euclidean distance  $l$  between the reflection points is just  $l = |2 \cos \beta| |\mathbf{v}|/|B| = |2p/B|$ , and that  $B < 0$  we obtain the result given in [18] for  $\beta < \pi/2$ . The above formula is also valid for the case of the outer billiard (e.g. outside the sphere, see [19]) with  $\beta > \pi/2$ . The stability diagram is the same as for the billiard without magnetic field given in Fig. 2.

### Harmonic oscillator

Let the potential be given by  $U(\mathbf{q}) = \omega^2 x^2/2 + \nu^2 y^2/2$ . The Jacobian of the flow is

$$\mathbf{M}(t) = \begin{pmatrix} \mathbf{C}_o & \mathbf{\Omega}^{-1}\mathbf{S}_i \\ -\mathbf{\Omega}\mathbf{S}_i & \mathbf{C}_o \end{pmatrix}, \quad (57)$$

with  $\mathbf{C}_o = \text{diag}(\cos \omega t, \cos \nu t)$ ,  $\mathbf{S}_i = \text{diag}(\sin \omega t, \sin \nu t)$ , and  $\mathbf{\Omega} = \text{diag}(\omega, \nu)$ . The general solution is  $X(t) = \mathbf{M}(t)X(0)$ . For a repulsive potential  $\omega, \nu$  are imaginary which leads to cosh and sinh instead of cos and sin. This system can have many different period one orbits. For periodicity we require  $\mathbf{q}(\tau) = \mathbf{q}_1 = (x_1, y_1)^t \neq 0$  where  $\tau$  is the (as yet undetermined) period of the orbit. The condition for a period one orbit reads

$$\mathbf{q}_1 = \mathbf{C}_o \mathbf{q}_1 + \mathbf{S}_i \mathbf{\Omega}^{-1} \mathbf{p}_1. \quad (58)$$

Excluding the special orbits with  $\det(\mathbf{1} - \mathbf{C}_o) = 0$  respectively  $\det \mathbf{S}_i = 0$ , we can solve for  $\mathbf{q}_1$ . Inserting into the corresponding solution for  $\mathbf{p}(\tau)$  gives the final momentum after time  $\tau$  again at the position  $\mathbf{q}_1$ ,

$$\mathbf{p}(\tau) = (-\mathbf{S}_i \boldsymbol{\Omega} (\mathbf{1} - \mathbf{C}_o)^{-1} \mathbf{S}_i \boldsymbol{\Omega}^{-1} + \mathbf{C}_o) \mathbf{p}_1 = -\mathbf{p}_1. \quad (59)$$

Because of  $\mathbf{p}(\tau) = -\mathbf{p}_1$  these orbits are self retracing: they go up the potential until they reach the oval of zero velocity and then return the same path in configuration space until they reach the initial point with reversed velocity. In order to obtain a period one orbit of the billiard the boundary at  $\mathbf{q}_1$  must be perpendicular to  $\mathbf{p}_1$ . This is the standard situation for billiards without magnetic field and we already encountered it for the period one orbit in the linear potential. By construction these orbits have time reversal symmetry. The normal  $\mathbf{n}$  at the point of reflection is parallel to  $\mathbf{p}_1$  and  $p = 0$ . Taking the trace of  $\mathbf{KM}$  we find

$$\text{tr}_1^{(4)} = 2 \cos 2\alpha (\cos \omega\tau - \cos \nu\tau) + \frac{R_{11}}{\omega} \sin \omega\tau + \frac{R_{22}}{\nu} \sin \nu\tau \quad (60)$$

with  $R_{ii}$  given by (36). For the calculation of  $\mathbf{R}$  note that  $\mathbf{n}$  is eigenvector of  $\mathbf{W}$  and  $\mathbf{v} \parallel \mathbf{n}$ , such that  $\mathbf{SW}\mathbf{v} = -\mathbf{S}\mathbf{v}$ . From (58) we obtain

$$\mathbf{p}_1 = \left( x_1 \omega \tan \frac{\omega\tau}{2}, y_1 \nu \tan \frac{\nu\tau}{2} \right)^t. \quad (61)$$

The relation between energy and period for fixed initial and final point  $\mathbf{q}_1$  is a transcendental equation,

$$h = \frac{x_1^2 \omega^2}{2 \cos^2 \omega\tau/2} + \frac{y_1^2 \nu^2}{2 \cos^2 \nu\tau/2}, \quad (62)$$

and therefore we leave everything parametrized by the period  $\tau$ . The divergence of the energy as a function of  $\tau$  is related to the fact that the period of oscillations in the harmonic oscillator is independent of the amplitude. The only variation in  $\tau$  comes from the fact that we do not start at the origin. If the energy is large, the difference in  $\tau$  due to this initial offset is relatively small and for infinite energy  $\tau$  approaches half the period  $\pi/\omega$  or  $\pi/\nu$ .

Now we study the orbits whose reflection condition  $\langle \mathbf{t}_1, \mathbf{p}_1 \rangle = 0$  with  $\mathbf{p}_1$  given by (61) is fulfilled independently of  $\tau$ , i.e. for which  $x_1 = 0$  or  $y_1 = 0$ . With an attractive potential the periodic orbits with small  $\tau$  run upwards in the potential. For  $\omega\tau$  or  $\nu\tau > \pi$  the initial momentum in the corresponding direction changes its sign, and the orbit goes down first, then up on the other side and returns to  $\mathbf{q}_1$ . Periods  $\tau$  larger than the full period don't give periodic orbits in the billiard. In a repulsive potential the orbit goes up in the direction of the origin because otherwise it would never return. The outer billiard with repulsive potential is a scattering system without periodic orbits. In the case  $y_1 = 0$  and  $x_1 > 0$  we obtain

$$\text{tr}_1^{(4)} = 4 \left( 1 \pm \frac{\omega}{\nu} \kappa x_1 \tan \frac{\omega\tau}{2} \tan \frac{\nu\tau}{2} \right) \cos^2 \frac{\nu\tau}{2}, \quad (63)$$

where  $\pm$  is the sign of the initial momentum. A similar expression holds for the case  $x_1 = 0$ .

In the case of the isotropic harmonic oscillator with  $\omega = \nu$  we get the simple expression

$$\text{tr}_1^{(4)} = 4 \cos^2 \omega \frac{\tau}{2} \pm 4 x_1 \kappa \sin^2 \frac{\omega\tau}{2}. \quad (64)$$

Introducing the energy  $h$  and  $U_1 = U(\mathbf{q}_1)$  gives

$$R = \left( 1 - \frac{U_1}{h} \right) (1 \mp \kappa x_1). \quad (65)$$

In the case that  $h = U_1$ , this describes a degenerate orbit which does not move at all. Let us first consider orbits with positive initial momentum. For larger  $h$  the orbit moves an

increasing distance radially outward. If the boundary is sufficiently defocusing ( $\kappa x < -1$ ) the orbit is always hyperbolic, while for slightly defocusing boundary with  $-1 < \kappa x < 0$  it is always elliptic. For a focusing boundary the orbit is stable for small energies and inverse hyperbolic for large energies. Note that the stability can be read off Fig. 2 with an appropriate reinterpretation of the axes. For orbits with initially negative  $x$ -momentum the sign of  $\kappa$  is defined with respect to the opposite normal, such that both orbits with either sign of the initial momentum have the same stability, despite the fact that one “sees” a focusing and the other one a defocusing boundary.

In a repulsive potential we have  $U_1 < h < 0$ . The upper bound on  $h$  ensures that the oval of zero velocity around the origin (which is needed for the period one orbit) does not vanish. We obtain the same stability formula, however now the minus sign in front of  $\kappa$  describes the (only possible) orbits with initial negative momentum.

The symmetric period two orbits can also be easily calculated, compare to the results in [9]. We start at  $(x_1, 0)$ ,  $x_1 > 0$  always with negative initial momentum until we reach  $(-x_1, 0)$ . Due to the assumed symmetry we can introduce a reflecting wall with curvature zero in the middle and for the symmetry reduced orbit in the attractive potential we find

$$R' = \left(1 - \frac{U_1}{h}\right)(1 - \kappa l/2) \quad (66)$$

and  $R = 4R'(1 - R')$  for the full orbit with  $l = 2x_1$  the distance between the reflection points. The factor  $1 - U_1/h$  is always positive and smaller than 1. Again the stability can be read off Fig. 2. For the repulsive potential we get the same formula, however, now it gives the complement of the residue for the symmetry reduced orbit

$$\bar{R}' = \left(1 - \frac{U_1}{h}\right)(1 - \kappa l/2) \quad (67)$$

and we obtain  $R = 4\bar{R}'(1 - \bar{R}')$  for the full orbit. The existence condition in the repulsive case is  $h > 0$ , such that the orbit can cross the potential hill at the origin. Therefore  $1 - U_1/h$  is always larger than 1.

P. Stifter [35] has shown that the ordinary billiard in the cardioid, which is ergodic [5], is equivalent to the billiard with repulsive potential  $-x^2 - y^2$  inside the unit circle with center  $(1, 0)$  for the energy  $H = 0$ . This is exactly the energy where the oval of zero velocity vanishes and there is an unstable equilibrium point at  $(0, 0)$ . Changing the energy gives a system which does not correspond to the cardioid billiard. Instead this gives an interesting example where a bounded system, which is close to integrable for low energies  $H \approx -4$  and high energies, is proven to be ergodic for the special intermediate energy value  $H = 0$ .

## 7 The rotating billiard

A rotating billiard, as introduced in [20], consists of an ordinary inner or outer billiard boundary that moves on a circle around the origin. If we study the outer billiard with two discs the system shows a striking similarity to the restricted three body problem, because in the latter system orbits with close encounters to either large body are effectively reflected, even though the gravitational force is attractive, such that the hard core potential of the billiard can model this motion. This special case of a rotating billiard will be referred to as the restricted three body billiard, abbreviated as R3BB. The Hamiltonian in a uniformly rotating frame of reference is given by

$$H = \frac{1}{2}\mathbf{p}^2 - \omega(xp_y - yp_x) = \frac{1}{2}(p_x + \omega y)^2 + \frac{1}{2}(p_y - \omega x)^2 - \frac{1}{2}\omega\mathbf{q}^2 \quad (68)$$

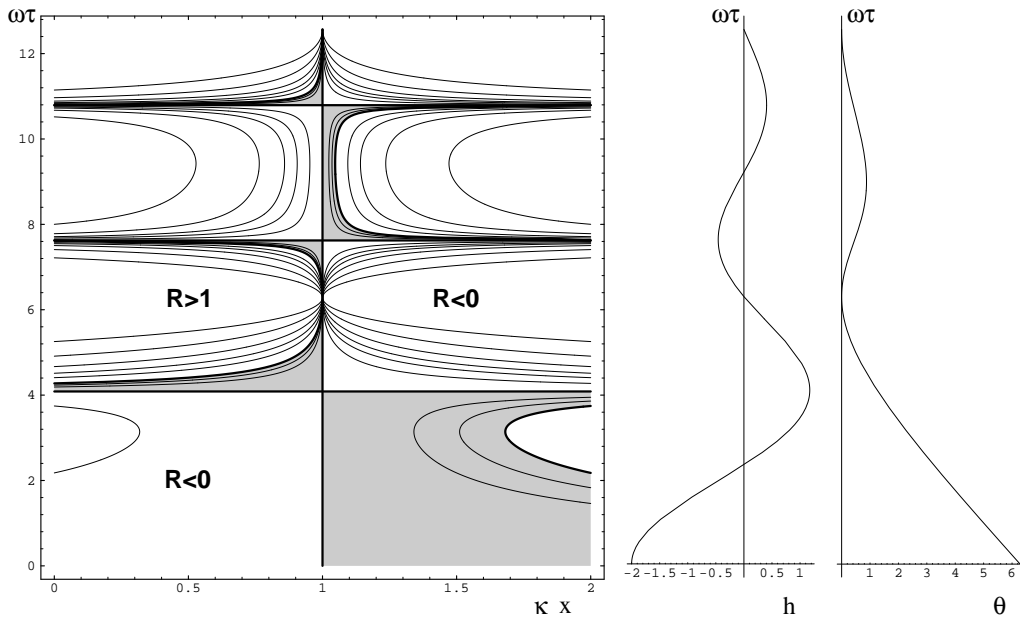


Figure 4: Stability diagram for the period one orbits in the R3BB as a function of  $\kappa x$  and  $\omega\tau$  as given by the residue  $R$  in (75). The elliptic region is shaded. Inside this region the lines with  $R = 1/2, 3/4$  are shown. In the unstable regions the residues  $-1, \pm 2, \pm 3, \pm 5, \pm 10, \pm 25$  and  $\pm 50$  are shown. The typical geometric situation is to the left of the vertical line  $\kappa x = 1$ , where the boundary is defocusing or only slightly focusing. We consider this region now: The horizontal lines indicate saddle center bifurcations. The retrograde orbit created at  $\omega\tau \approx 4.08$  is stable for slightly larger period, similarly the other retrograde orbits with  $\omega\tau \approx (2m + 1 + 1/2)\pi$ , for which  $h > 0$ . The direct orbits ( $h < 0$ ) bifurcating at  $\omega\tau \approx (2m + 1/2)\pi$  are stable for slightly smaller period. The infinite residues at  $\omega\tau = 2m\pi$  prevent the smooth continuation of a retrograde orbit to another retrograde orbit, similarly for the direct orbits. In the left two pictures the energy  $h$  and the angle  $\theta$  between in- and outgoing velocities at the reflection point as a function of  $\omega\tau$  are shown.

such that we have a harmonic repulsive potential  $U = -\omega\mathbf{q}^2/2$  and a vector potential  $\mathcal{A} = (-\omega y, \omega x)^t$ . The Jacobian of the free motion is

$$\mathbf{M}(t) = \begin{pmatrix} \mathbf{D}(\omega t) & t\mathbf{D}(\omega t) \\ \mathbf{0} & \mathbf{D}(\omega t) \end{pmatrix}, \quad (69)$$

such that the general solution can be written as  $X(t) = \mathbf{M}(t)X(0)$ . In the context of the restricted three body problem the analog of the above Hamiltonian is referred to as the Jacobi integral; we will stay with the former name and also call the value of the Hamiltonian the energy, which is *not* the energy of the particle in the non rotating frame. In rotating coordinates the discs are fixed on the  $x$ -axis at some distance from the origin. The straight line motion looks rather (nice and) complicated in the rotating frame of reference. The free motion is circle-like due to the coriolis field but it is somewhat distorted due to the repulsive harmonic potential centered at the origin. Depending on the value of the Hamiltonian there can be up to an infinite number of period one orbits coexisting. Now we are going to calculate the stability of these orbits.

To have a solution that returns to  $\mathbf{q}_1 \neq 0$  after time  $\tau$  we must choose the initial momenta according to  $\mathbf{q}_q = \mathbf{q}(\tau)$  and with (69) this gives

$$\mathbf{q}_1 = \mathbf{D}(\omega\tau)\mathbf{q}_1 + \tau\mathbf{D}(\omega\tau)\mathbf{p}_1. \quad (70)$$

The final momenta are  $\mathbf{p}(\tau) = \mathbf{D}(\omega\tau)\mathbf{p}_1$  and the angle  $\theta$  between the initial and final velocities  $\mathbf{v} = \mathbf{p} - \mathcal{A}(\mathbf{q}_1)$  is given by

$$\cos \theta = 1 - 2 \frac{(1 - \cos \omega\tau)^2}{2 - 2 \cos \omega\tau - 2\omega\tau \sin \omega\tau + \omega^2\tau^2}. \quad (71)$$

For  $\omega\tau = 2\pi m$ ,  $m = \pm 1, \pm 2, \dots$ ,  $\theta$  is zero such that the free motion is periodic by itself; in the non rotating frame the particle does not move at all. This is similar to the ordinary billiard, where an orbit touching the boundary becomes infinitely unstable due to  $n \rightarrow 0$ . For every other value of  $\tau$ , however, a periodic orbit of the billiard exists. The angle between the normal at the reflection point and the velocity in the non rotating frame (!) is given by  $\vartheta = (\pi - \omega\tau)/2 \bmod \pi - \pi/2$ . For negative  $\vartheta$  the velocity is directed against the direction of rotation of the disk (retrograde), while for positive  $\vartheta$  the direction is the same (direct). Retrograde orbits typically have higher energy than direct orbits because they have to be faster to reach the next collision. The energy for these periodic orbits parametrized by  $\tau$  is obtained by eliminating  $\mathbf{p}$  in (68) using (70),

$$h = \frac{r^2}{\tau^2}(1 - \cos \omega\tau - \omega\tau \sin \omega\tau), \quad (72)$$

which is shown in Fig. 4, where  $|\mathbf{q}_1| = r = 2$ . Every intersection of the line  $h = \text{const}$  with this curve corresponds to a periodic orbit of the system. At extrema of this curve periodic orbits are created/destroyed in pairs when the energy is varied. At maxima retrograde orbits bifurcate and at the minima direct orbits bifurcate. These important points are given by

$$h' = \frac{\partial h}{\partial \tau} = -\frac{r^2}{\tau^3}(2 - 2 \cos \omega\tau - 2\omega\tau \sin \omega\tau + \omega^2\tau^2 \cos \omega\tau) \stackrel{!}{=} 0, \quad (73)$$

which will turn out to be closely related to the stability.

Taking the trace of  $\mathbf{KM}$  we find the general stability formula to be

$$\text{tr}_1^{(4)} = \tau (\cos \omega\tau (R_{11} + R_{22}) + \sin \omega\tau (R_{21} - R_{12})), \quad (74)$$

and for the use of (38) we need  $\langle \partial_q U, \mathbf{n} \rangle = \omega^2(x_1 \sin \alpha - y_1 \cos \alpha)$  and  $B = -2\omega$ . In order for the reflection to map  $\mathbf{v}(\tau)$  into  $\mathbf{v}(0)$  we must have  $\langle \mathbf{p}(\tau) - \mathcal{A}(\mathbf{q}_1), \mathbf{t}_1 \rangle = \langle (\mathbf{p}_1 - \mathcal{A}(\mathbf{q}_1), \mathbf{t}_1) \rangle$ , which gives  $\alpha_1 = \arctan(x_1/y_1)$ . We now choose a coordinate system in such a way that the orbit starts at  $y_1 = 0$ , such that  $\alpha_1 = \pi/2$  and  $\mathbf{D} = \mathbf{S}$ . Introducing the distance from the origin  $r = x_1$  the residue obtained from (74) is

$$R = \frac{1}{2} \frac{2 - 2 \cos \omega\tau - 2\omega\tau \sin \omega\tau + \omega^2\tau^2 \cos \omega\tau}{\cos \omega\tau - 1} (r\kappa - 1) \quad (75)$$

$$= (\omega^2\tau^2/2 - \frac{\cos \omega\tau - 1}{\cos \theta - 1})(r\kappa - 1) \quad (76)$$

$$= h' \frac{\tau^3}{2r^2} \frac{r\kappa - 1}{1 - \cos \omega\tau}. \quad (77)$$

The last formula nicely illustrates the saddle-center bifurcations at the extrema of  $h(\tau)$ : Two new orbits are created with stability  $R = 0$ , i.e.  $h' = 0$ , which is just the condition for the bifurcation. Close to the bifurcation point  $h'$  has different signs for the two orbits, such that one is elliptic and the other one direct hyperbolic. The elliptic orbit becomes inverse hyperbolic typically after only a slight change of  $\tau$ . The interval of stability decreases with increasing  $\tau$ . The whole scenario is illustrated in the stability diagram of Fig. 4, which completes the results reported in [20].

As our final application we now turn to the calculation of the period two orbits in the R3BB, which are of great interest because of their apparent similarity with orbits in the restricted three body problem that have close encounters with both centers. We treat the symmetric case with  $\kappa = \kappa_i$  and  $\mathbf{q}_1 = (r, 0)$  and  $\mathbf{q}_2 = (-r, 0)$ . The analogue of (70) gives  $\mathbf{p}_1$  for the given  $\mathbf{q}_1$  and  $\mathbf{q}_2$ . The resulting energy is

$$\tilde{h} = \frac{r^2}{\tau^2}(1 + \cos \omega\tau + \omega\tau \sin \omega\tau). \quad (78)$$

The main difference to the period one orbits is that  $\tilde{h}$  diverges for  $\tau \rightarrow 0$ . Therefore we have a period two orbit up to infinite energies, which bounces back and forth between the two disks with the motion becoming a straight line for  $\tau \rightarrow 0$  and  $\tilde{h} \rightarrow \infty$ . Except for this behavior we again have the oscillations in  $\tilde{h}(\tau)$  and therefore a bifurcation scenario similar to that of the period one orbits. The important features of the residue again depend on the derivative of  $\tilde{h}$ , which is given by

$$\tilde{h}' = \frac{\partial \tilde{h}}{\partial \tau} = -\frac{r^2}{\tau^3} (2 + 2 \cos \omega \tau + 2 \omega \tau \sin \omega \tau - \omega^2 \tau^2 \cos \omega \tau). \quad (79)$$

Because of the above symmetry assumptions the **t-n**-coordinates are given by  $\alpha_1 = \pi/2$  and  $\alpha_2 = 3\pi/2$  such that  $\mathbf{K}_1 = \mathbf{K}_2$  with  $\mathbf{W}_1 = \mathbf{W}_2 = \mathbf{W}_0$ . Although the orbit is not time reversal symmetric we have  $\tau = \tau_1 = \tau_2$  due to the spatial symmetry and therefore  $\mathbf{M}_1 = \mathbf{M}_2$ . For the trace of **KMKM** we find

$$\text{tr}_2^{(4)} = 4(2\bar{R}' - 1)^2, \quad \bar{R}' = \tilde{h}' \frac{\tau^3}{2r^2} \frac{r\kappa - 1}{1 + \cos \omega \tau}, \quad (80)$$

giving the same factorization of  $\bar{R} = \text{tr}_2^{(4)}/4$  as in the gravitational billiard (54).

The bifurcation scenario for the period two orbits is as follows. They are created in saddle center bifurcations at the extrema of  $\tilde{h}$ . The residue of the elliptic orbit increases from 0 to 1. However the residue does not increase beyond 1 but instead begins to decrease again. This “touching of residue 1” is an effect of the symmetry of the orbit, which corresponds to passage of  $R'$  through  $1/2$ . There are two period four orbits involved in this  $2/4$ -bifurcation [30] and the old orbit stays elliptic. Eventually it reaches  $R = 0$  again and loses stability in a period doubling bifurcation. For retrograde orbits this scenario happens for decreasing period  $\tau$ , and for direct orbits with increasing period. Decreasing the period of the retrograde orbits further eventually turns them infinitely unstable at  $1 + \cos \omega \tau = 0$ , where they have a tangency instead of a reflection. The same happens for the direct orbits if we increase their period. However, if we increase the period of a retrograde orbit it becomes more and more unstable, but eventually becomes direct and then stable again, thus every two of the orbits described above are continuously connected in phase space. The whole scenario is repeated for any number  $m$  of revolutions that are completed in the non rotating frame before the next reflection. The intervals of stability are extremely small for higher periods. Only in the case  $\kappa r \approx 1$ , i.e. the distance from the origin is close to the radius of curvature, are the windows of stability larger. For  $\kappa r = 1$  all the orbits become inverse parabolic, independently of the period. Note that this case is completely different from the standard case in the R3BB, because the curvature must be positive. As a matter of fact, the case  $\kappa r = 1$  can be realized as an orbit *inside* a circle, and we reobtain the integrable circle billiard described in rotating coordinates. The distance between the reflection points of the orbit is  $l = 2r$ , such that the same geometric factor enters the residue as in the previous examples.

It is possible to treat the general period two orbit, with different curvatures and distances from the origin. This case is quite promising in order to make a more quantitative comparison with the restricted three body problem, because with these parameters we have an analog of the mass ratio in our system. In any case the system at hand, which was introduced in [20], gives the opportunity to obtain analytical stability results. This tempers the feeling that this approximation of the three body problem is too crude, and we hope, as cited in the beginning, that “only the interesting qualitative questions need to be considered”.

## 8 Conclusion

We have derived a general expression for the linearized Poincaré map in a billiard with potential. Due to the additional coupling introduced by a (vector) potential the linearized

map can only conveniently be written in four dimensions. Using a canonical transformation in phase space we have calculated the linearization and it turned out that the arc length and the parallel component of the velocity (not of the momentum) give a canonical coordinate system on the surface of section given by the billiard boundary. This holds true for any potential. The resulting formula is useful for the application of numerical methods to find periodic orbits, or for the estimation of the Lyapunov exponent. Moreover, since the linearization in phase space includes the variation of the energy, which usually gives a nontrivial change in the orbit for a billiard with potential, it can also be used to follow periodic orbits when the energy is varied.

The main application of the linearized map is the calculation of the stability of periodic orbits. The trace of the (four dimensional) monodromy matrix of the periodic orbit can be factorized into a product of matrices describing the piecewise free motion between reflections and the contribution from the reflection. This generalizes a well known formula with  $2 \times 2$  matrices for ordinary billiards. With these results it was possible to perform the stability analysis of period one and two orbits in four billiards with different (vector) potentials.

The results are presented in form of stability diagrams, where the residue of the orbits is shown in its essential parameter dependence. These diagrams can give some intuition about the mechanisms that create stability respectively instability. The investigation of stability diagrams of the ordinary billiard (which is the same as for the one with magnetic field) and the gravitational billiard showed that periodic orbits in one parameter families of integrable systems tend to avoid period doubling bifurcations which are generically present. In the final application to a rotating billiard, which mimics the restricted three body problem, we have obtained an interesting bifurcation scenario of an infinite number of period one and two orbits by successive saddle-center bifurcations with increasing period. The calculations for this system can be extended to the non-symmetric case, in order to obtain a simple system that presents some essential features of the restricted three body problem in an analytically tractable way.

## Acknowledgement

The author would like to thank A. Wittek, P.H. Richter, H.-P. Schwebler, and A. Bäcker for helpful discussions. This work was supported by the Deutsche Forschungsgemeinschaft.

## References

- [1] G. D. Birkhoff, *Dynamical Systems* (American Mathematical Society, Providence, RI, 1927).
- [2] Y. F. Lazutkin, *Izv. Acad. Sci. Ser. Math.* **37**, 186 (1973).
- [3] Y. G. Sinai, *Russ. Math. Surveys* **25**, 137 (1970).
- [4] L. A. Bunimovich, *Commun. Math. Phys.* **65**, 295 (1979).
- [5] M. P. Wojtkowski, *Commun. Math. Phys.* **105**, 391 (1986).
- [6] G. Benettin and J.-M. Strelcyn, *Phys. Rev. A* **17**, 773 (1978).
- [7] M. V. Berry, *Eur. J. Phys.* **2**, 91 (1981).
- [8] M. Hénon and J. Wisdom, *Physica* **8D**, 157 (1983).
- [9] V. V. Kozlov and D. V. Treshchev, *Billiards – A Genetic Introduction to the Dynamics of Systems with Impacts* (American Mathematical Society, Providence, RI, 1991).

- [10] H. R. Dullin, P. H. Richter, and A. Wittek, *Chaos* **6**, 43 (1996).
- [11] H. E. Lehtihet and B. N. Miller, *Physica* **21D**, 93 (1986).
- [12] P. H. Richter, H.-J. Scholz, and A. Wittek, *Nonlinearity* **3**, 45 (1990).
- [13] T. Szeredi and D. A. Goodings, *Phys. Rev. E* **48**, 3518 (1993).
- [14] S. A. Chaplygin, *Complete Collections of Works, Vol. 1* (Izd.Akad.Nauk SSSR, Leningrad, 1933), pp. 194–199, (in Russian).
- [15] A. Hayli and A. Vidović., *Lecture Notes in Physics* **430**, 85 (1994).
- [16] H. J. Korsch and J. Lang, *J. Phys. A: Math. Gen* **24**, 45 (1991).
- [17] C. G. J. Jacobi, *Vorlesungen über Dynamik* (Chelsea Publ., New York, 1969).
- [18] M. Robnik and M. V. Berry, *J. Phys. A: Math. Gen.* **18**, 1361 (1985).
- [19] N. Berglund and H. Kunz, *J. Stat. Phys.* (1996).
- [20] N. Meyer *et al.*, *J. Phys. A: Math. Gen.* **28**, 2529 (1995).
- [21] H. R. Dullin and A. Wittek, *J. Phys. A* **28**, 7157 (1995).
- [22] R. Abraham and J. E. Marsden, *Foundations of Mechanics*, 2 ed. (Benjamin-Cummings, Reading, MA, 1978).
- [23] M. C. Gutzwiller, *Chaos in Classical and Quantum Mechanics*, Vol. 1 of *Interdisciplinary Applied Mathematics* (Springer, Berlin, 1990).
- [24] K. R. Meyer and G. R. Hall, *Introduction to Hamiltonian Dynamical Systems and the N-Body Problem* (Springer, Berlin, 1992).
- [25] A. Bäcker and H. R. Dullin, DESY Preprint 95-198, ChaoDyn 10/9511004, submitted to *J. Phys. A.* (1995).
- [26] S. C. Creagh, J. M. Robbins, and R. G. Littlejohn, *Phys. Rev. A* **42**, 1907 (1990).
- [27] M. Sieber and F. Steiner, *Physica* **D44**, 248 (1990).
- [28] B. Eckhardt and D. Wintgen, *J. Phys. A* **24**, 4335 (1991).
- [29] J. M. Greene, *Journal of Mathematical Physics* **20**, 1183 (1979).
- [30] J. M. Greene, R. S. MacKay, F. Vivaldi, and M. J. Feigenbaum, *Physica* **3D**, 468 (1981).
- [31] R. J. Rimmer, *Mem. AMS* **41**, (1983).
- [32] K. Meyer, *Trans. Am. Math. Soc.* **149**, 95 (1970).
- [33] M. Hénon, *Physica* **33D**, 132 (1988).
- [34] M. P. Wojtkowski, *Commun. Math. Phys.* **126**, 507 (1990).
- [35] P. Stifter, (private communication) (unpublished).